Optimization of the Compression-Based Piezoelectric Traffic Model (CPTM) for Road Energy Harvesting Application

Saleh Gareh*‡, B. C. Kok*, M. H. Yee**, Abdoulhdi. A. Borhana ***, S. K. Alswed*

(salehgareh@gmail.com ,bckok@uthm.edu.my, mhyee@uthm.edu.my, amhmad@uniten.edu.my, sageralswed@gmail.com)

*Department of Electrical Power Engineering, Faculty of Electrical & Electronic Engineering, UTHM 86400, Johor, Malaysia.

**Faculty of Technical and Vocational Education, Universiti Tun Hussein Onn Malaysia.

***Department of Mechanical Engineering, College of Engineering, Universiti Tenaga Nasional, 43000 Kajang, Selangor Darul Ehsan.

‡Corresponding Author; Saleh Gareh, Department of Electrical Power Engineering, Faculty of Electrical & Electronic Engineering, UTHM 86400, Johor, Malaysia, salehgareh@gmail.com

Received: 16.05.2019 Accepted:17.06.2019

Abstract- This paper employs the Two-Degree-of-Freedom (2DOF) electromechanical model to show the probability of the piezoelectric approach as an option for energy scavenging devices in roadway applications. The passing vehicles are the main energy source for harvesting device. A 2DOF electromechanical model as the piezoelectric harvesting unit is applied to explain the harvester performance in a single lane road. APC piezoelectric ceramic (APC 855) is selected as the optimum piezoelectric material due to its high piezoelectric constant values and high piezoelectric charge constant. Also, in the traffic model, we employ a Cellular Automata (CA) model. The vehicle dynamics model is used to transfer information from the traffic model to the piezoelectric model. Combining both the traffic model, i.e. the piezoelectric and the vehicle dynamics model, results in the compression-based piezoelectric traffic model (CPTM). In a single-lane traffic model with different arrival rate λ, a single circle-shaped Piezoelectric Cymbal Transducer (PCT) with thickness of 0.3 mm and diameter of 32 mm is applied, in which the produced power is 14.126 W and 29.746 W and 6.47 W. Based on these outcomes, if we lay multiple PCT arrays along the highway road, a large amount of power can be produced. Hence, a great potential is shown by the proposed electromechanical-traffic model for applications related to the macro-scale roadway electric power generation systems.

Keywords Piezoelectric Energy Harvester; Mean Arrival Rate; 2DOF; Cellular Automata (CA); PCT.

1. Introduction

Recently, several studies have been conducted to enhance the range of renewable energy from environmental resources such as extracting, converting, and storing power from motion, pressure, temperature or vibration derived from rain, waves, wind, light, tides, etc. The enhancements include developing of innovative materials and methods to gather and convert extremely small amounts of energy from the environment into electrical energy. This area attracting the researchers interest to develop more ways of using energy harvesting technologies to generate power [1-3]. For instance, Vibration based energy include ordinary household appliances, vehicles, machines, street traffic, acoustic vibrations and beside many others [4-10] become an interested field for researchers in order to generate small amounts of energy to be used for different applications. Vibration energy scavenging or harvesting is generally the process of harnessing power from ambient vibration sources. Different methods, such as electrostatic generation, electromagnetic induction and piezoelectric generation, can be employed for harvesting electrical energy through external vibrations [11]. Different tools and materials are used for generating electrical power (energy harvesting) from vehicles movements and pressures. Piezoelectricity is a common tool which can transform electrical energy into mechanical energy reverse. Pierre Curie (1859-1906) and Jacques Curie (1856-1941) discovered and developed the initial theory on piezoelectricity which is by compressing some crystals in certain directions, positive charges and negative charges could be generated on certain sections of the surface [12]. Since the first piezoelectricity theory is released, the need for alternative

ways to generate electricity became a challenge to many countries. Solar energy or other mechanical energy could be considered as few of the alternative sources for electricity. Also, air or water flow could be harnessed to create moving objects or vibrating structures, which form the main sources of mechanical energy. However, there is a noticeable growth and extreme demand become in generating electricity form more suitable and friendly environmental resources. Such resources are environment and are much cheaper when compared to conventional energy technologies. Although, intensive studied on three different types of generating electricity mechanisms from vibration include piezoelectric, electromagnetic and electrostatic. However, piezoelectric energy harvester is one of the most important applications among several applications of vibration, Relatively there are a few studies have addressed but there are minority studies related to piezoelectric energy harvesters [13]. The method allows generating electric energy by employing the force of vehicles due to gravity by making use of deformations in the paving materials [14].

Several researches have been carried out and studies have been presented to discuss the harvesting of energy from ambient sources such as heat, wind, solar, radio frequency radiations, and vibrations [15-23]. The focus of these studies have been to explore how these energy sources can replace or supplement the existing sources of energy such as batteries, and provide renewable, clean and sustainable energy for wireless sensor networks (WSNs). Some of the energy harvesting enablers include wind turbines, thermoelectric generators, photovoltaic cells, and mechanical vibration set-ups such as electromagnetic and piezoelectric machineries [24]. Table 1 shows the contemporary energy harvesting facilitators or enablers, and their energy harvesting mechanisms and power generation capabilities.

Table 1. Various harvesting methods and their power generation densities [7]

Harvesting Method	**Power Density** ($\mu W/cm^3$)
Solar Cells (Outdoors)	1500 - Direct sun, 150 - Cloudy day
Solar Cells (Outdoors)	6
Vibration (electrostatic conversion)	50
Vibrations (piezoelectric conversion)	250
Thermoelectric	10

The table above shows that the harvesting schemes of solar cells (which perform effectively in direct sunlight) and the piezoelectric model stand far above other models in terms of power generation density. However, the existing models for the harvesting of piezoelectric energy have not been used with traffic models, which give the real picture of such applications.

This article focuses on theoretical and simulation studies of a compression-based piezoelectric energy harvester. The study also employs a Cellular Automata (CA) model in the traffic model to calculate the generated power and voltage of the developed model. According to [25], in compression configuration, the use of piezoelectric harvester would be more frangible in large force vibration environments like the large compressive loadings that are stimulated by heavy trucks on the pavement as shown in Fig 1. The related terms associated with the direct piezoelectric effect in piezoelectric materials include the sensor effect and generator effect, while terms like actuator effect and motor effect are more related to the piezoelectric materials' converse piezoelectric effect. In most cases, the use of direct piezoelectric effect is for energy harvesting, a process of taking out energy from the environment, which are converted into electrical energy and stockpiled [26].

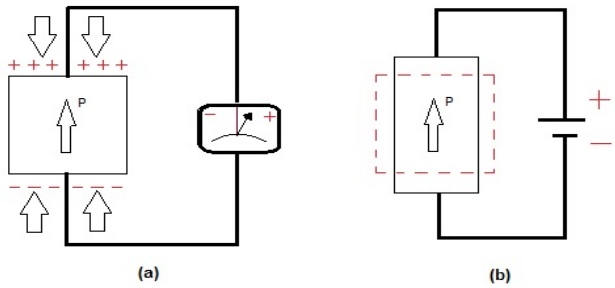

Fig 1. (a) Direct piezoelectric effect, (b) Converse piezoelectric effect [1]

As the process of conversion of mechanical strain into electricity by piezoelectric materials has high power density, lower cost, and relatively simple structure, it has been the focus of the recent research. Fig 2 presents the conventional energy harvester (CEH) that characteristically constitutes of a piezoelectric element, packed in between a base subjected to sinusoidal excitation and a proof mass.

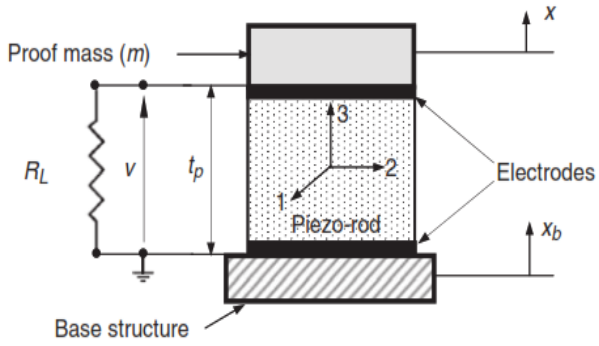

Fig 2. Conventional energy harvester [27].

The study has been [27] conducted on multiple-degree-of-freedom (DOF) models of cantilevered piezoelectric. A novel multiple-DOF harvesting model of the cantilevered piezoelectric harvester has been presented in [28], and the equivalent circuit of n-DOF to construct a harvester with multiple peaks has been developed to improve the magnitude. In addition, the authors in [29] introduced a nonlinear two-degree-of-freedom (2-DOF) model of the cantilevered piezoelectric harvester to augment the performance of the piezoelectric energy harvesters. The authors in [30] discussed

the use of a cantilever piezoelectric harvester to channelize and accumulate the energy generated by traffic movement over bridges in the form of vibrations. At the end of the exercise, the power harvested amounted to almost 0.03 mW, where the voltage was kept between 1.8 and 3.6 V with frequency not going beyond 15 Hz. Furthermore, [31] a power of 85 mW was derived from direct current DC using module of 36 layers under excitation with a frequency of 6 Hz and force amplitude of 1,360 N. In a similar manner, the authors in [32] analysed the energy harvesting potential of piezoelectric-based materials through the use of piezoelectric cantilever-based harvesters in civil infrastructures. Based on the simulation result, with smaller bridge span lengths and poorer road conditions, the energy output power was observed to increase. Moreover, the output power generated could fulfil or quench the minimum power demand required by sensor nodes. Recently, the authors in [33] experimented on a road energy harvester by using a Model Mobil Load Simulator (MMLS3) and a Universal Testing Machine (UTM). The maximum voltage and power of the developed harvester were 75.7 V and 280 mW, respectively.

Although there are several attempts by [25, 27, 30-34] that employed piezoelectric for energy harvesting, however, the generated and the obtained power was very low as it measured by a microwatt [35]. A piezoelectric harvester system comprises two basic elements: the mechanical component that generates electrical energy and an electrical circuit that converts and rectifies the energy generated as an alternating voltage to a constant voltage. The effectiveness of the energy harvester design is not only dependent on the piezoelectric harvester but also on its integration with the electrical circuit. Hence, to optimise the design as well as for comprehending the behaviour of the piezoelectric harvester, the use of an electromechanical model is of utmost importance that takes into account both the mechanical and electrical aspects of the recommended harvester [36]. For the roadway energy harvester, the use of a compression-based piezoelectric model has been proposed in this paper. Every single compression cycle generates energy in the form of pulses under the dynamic forces of compression.

2. Methodology

In this section, the models that are used and the simulation procedure are illustrated and explained. The proposed model compression based piezoelectric traffic model (CPTM) requires a collaboration of three models to be effective in modelling a real-life scenario of a compression based energy harvesting system. The models involved are the traffic model, vehicle dynamics model and piezoelectric model as shown in fig 3. The traffic model enables the simulation of traffic on the road. This provides the set of vehicles that interact with the piezoelectric model to generate the voltage and power to the energy harvesting system. The vehicle dynamics model connects the traffic model and the piezoelectric model such that the movement of vehicle from the former is properly reflected.

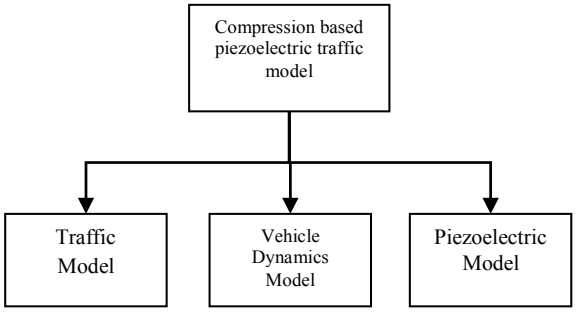

Fig 3. Involved models to simulate real-life scenario of a compression based energy harvesting system.

In the traffic model we considered 100 cells and the vehicles moved from one cell to another based on the rules defined within the traffic model. When a vehicle passed over the piezoelectric cells, the piezoelectric model is activated. The information from the traffic model was passed to the piezoelectric model via the vehicle dynamics model. The voltage and power of the moving vehicle were then calculated. After the vehicle left the piezoelectric cell, it continues in the movement until the end of the traffic model. Once it reached the last cell, the vehicle is then removed from the traffic flow. These processes are repeated until the current time exceeded the maximum predefined time. It is worth to mention that, all the micro-processes within the simulation are naturally automatic in the sense that they proceeded without any intervention from the user. The Control is enabled only through the configuration file prior to the initiation of the simulation.

2.1. Simulation Procedure

The simulation part is applicable only for collision-free and non-congested traffic conditions. An assumption is made that all the vehicles in the road traffic have identical features, wherein the vehicles possess two axles and their masses do not have significant variance from one another. Also, another assumption is made according to which the speed of the vehicles can either be fixed and or arbitrarily assigned. Fig 4 presents the general flow of the simulation process carried out through JAVA programming, and it is often the preferred language for most traffic simulating models.

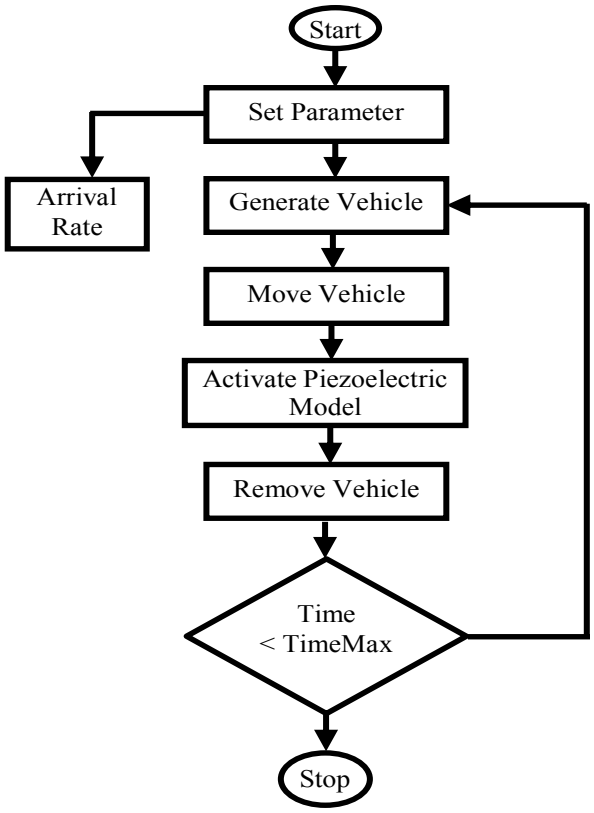

Fig 4. General Simulation Procedure.

The simulation began with the configuration of the involved models. The parameters were set in accordance with the portion of reality to be modelled. One of the most important parameters for a traffic model is the mean arrival rate (λ), which determines the flow of traffic as well as the traffic density. In this simulation, three rates were considered λ = 1, 0.5 and 0.1 which corresponded to high traffic, medium and low traffic, respectively. However, to study the possibility of optimal power generation, the simulation was defined based on the mean arrival rate and resistance. Different series of arrival rates (λ) at the traffic model, and resistances (kΩ) at the piezoelectric model are manipulating then the overall power generated over the period of three hours was carefully analysed.

2.2. Piezoelectric model

The traffic model interacts with piezoelectric model. In the model it is recommended an external intervention that stimulates the attainment of the optimal frequency. Therefore, the target of the model is to realize a near optimal situation for energy harvesting. Figure 5 shows the incremental refinement of the model with three variations namely; Basic, Extended and Optimal Frequency. The first variation, or basic model is a consequence of the first cycle. Whereby the extended model comes from the second cycle and the final model is a result of the third cycle. Refining the model incrementally is a strategic effort of minimizing the occurrence of error. The main idea of doing such a model is to evolve with proper stability.

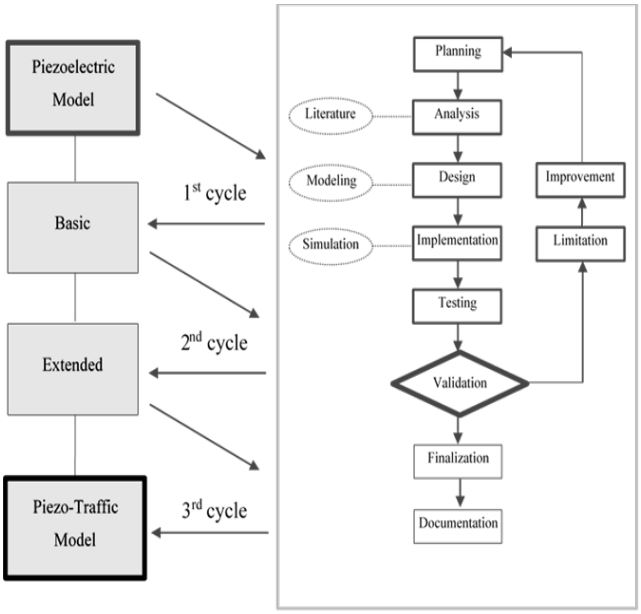

Fig 5. Incremental Refinement of Model.

The chosen piezoelectric model for conducting this simulation is two-degree-of-freedom model (2DOF) which is developed by [25]. This model can be embedded into the civil building, roads, and highways to harvest electrical energy. The model consists of electrical and mechanical properties. The Piezoelectric Cymbal Transducer (PCT), which is shown in Fig 6 and the electromechanical model, which is shown in fig 7). The piezoelectric cymbal expected to produce an electric charge and convert external kinetic energy into electricity.

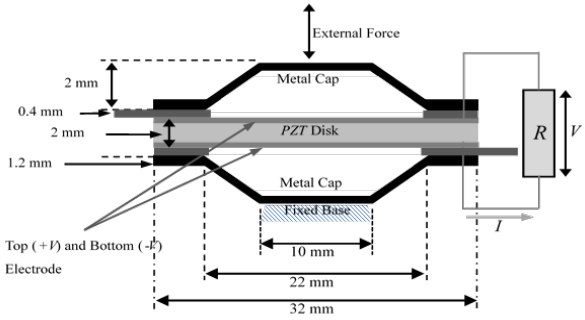

Fig 6. Piezoelectric Cymbal Transducer (PCT) [37].

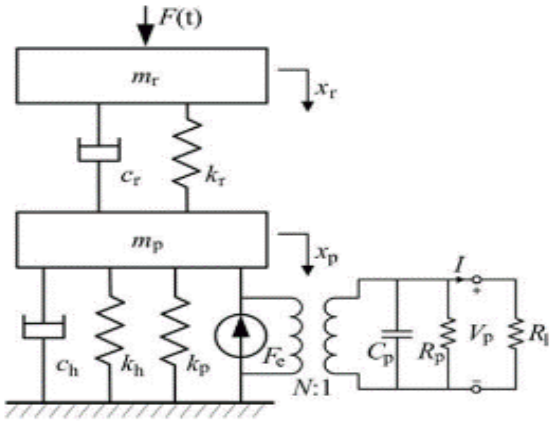

Fig 7. Electrical and mechanical properties of piezoelectric model [25].

The general properties of the selected piezo is presented in Table 2, which is shared by the APC piezo ceramic materials.

Table 2. Properties of the piezoelectric materials

Property	APC 840	APC 855	APC 880
$d_{33}[pm/V]$	290	630	215
K_{33}	0.72	0.76	0.62
$\varepsilon_{33}^{T}/\varepsilon_0$	1000	3800	1800
Q_m	500	65	1000

The electromechanical-traffic model has been developed with a single cell of the piezoelectric that constitutes of a poled piezoelectric disk (completely covered with electrodes on the top and bottom surface). The piezoelectric model's parameters are depicted in Table 3.

Table 3. Piezoelectric Parameters used in simulation part

Parameter	Symbo	Value
mass of metal cap layer	mr	0.0330
damping of metal cap layer	cr	0.0300
elastic coefficient of metal cap	kr	570000
deformation of metal cap layer	xr	0.1000
mass of piezoelectric material	mp	0.1220
elastic coefficient of piezoelectric	kp	270000000
Damping of mechanical structure	ch	5.1000
elastic coefficient of mechanical	kh	275000000
electromechanical conversion	N	0.7600
Capacitor	Cp	0.00000007

2.3. Traffic Model

Different traffic models could be found in several studies. However, in this study the researcher exploited the traffic model proposed by [38, 39] which employs cellular automata [40] to model complex behavior of traffic on a discrete timeline. The main aim of traffic model is to simulate overall movements of the vehicles which are passing over the piezoelectric harvester. A simple example for the traffic model is given in Fig 8. whereas Fig 9 shows a car when it is speeding with acceleration *a* on. The traffic model essentially provides the velocity (v) of the vehicle where it is possible to calculate the vertical force (Fz) of the front tire (FZ1) and rear tire (FZ2) with the road [41]. This requires the mass of the vehicle (m), gravity (g), wheelbase (l), distance between center of gravity (COG) to the front tire (l1), rear tire (l2) and ground (h), as well as the acceleration (a) of the vehicle.

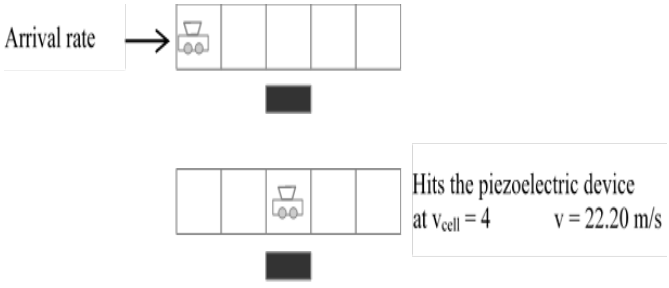

Fig 8. An accelerating car on a level pavement [41]

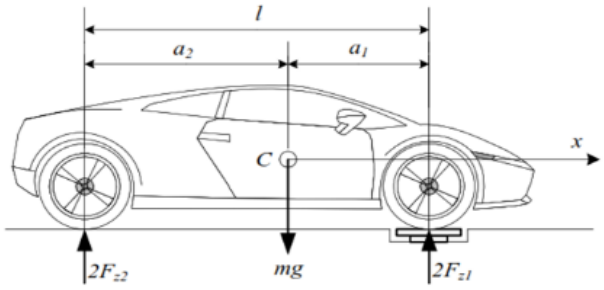

Fig 9. Simple Example for the Traffic Model

The forces are different for the front (Fz1) and back tire (Fz2) due to the dimension of the vehicle which directly effect on the center of gravity. The vertical forces under the front and rear wheels are:

$$F_{z1} = \frac{1}{2}mg\frac{a_2}{l} - \frac{1}{2}mg\frac{h}{l}\frac{a}{g} \quad (1)$$

$$F_{z2} = \frac{1}{2}mg\frac{a_1}{l} + \frac{1}{2}mg\frac{h}{l}\frac{a}{g} \quad (2)$$

Where, *a* acceleration, F_{z1} normal force under front wheels, F_{z2} normal force under rear wheels, l wheel base, m car mass, a_1 distance of first axle from mass centre, a_2 distance of second axle from mass centre, C mass centre of vehicle, h height of C and ***g*** gravitational acceleration. The average specifications for two axles vehicle is shown in Table 4 [42].

Table 4. The average characteristics of a vehicle

Specification	Value
Weight [Kg]	1500
Center of Gravity (CG) height h [m]	0.7
l Wheelbase [m]	2.5
a_1 [m]	1.3
a_2 [m]	1.2

The input for the piezoelectric model is gained from the traffic model which represented by the force *F(t)* caused by the vehicle. The traffic model must be devised, and the simplest case would be a single lane simulation by considering the flow of traffic [43] which emulates a possibly linear traffic with multiple lane. In this study, the main assumptions in the traffic model are that:

1. The maximum speed is 120km/h and there are 6 total discrete values of cell velocity.
2. The Arrival of vehicle as determined by the Poisson distribution.
3. The Traffic flow causes the vehicle to accelerate to decelerate.
4. The Vehicle hits the PCT twice to activate the piezoelectric. Since there are two separate vertical forces

from the front tires (F_Z1) and rear tires (F_Z2). The vertical forces are calculated by using the equations (1), (2).

2.4. Vehicle Dynamics Model

The vehicle dynamic model simulates the vehicle structure and states. Thus, studying the impact of the movement is essential to analysing the transfer of force and velocity between the vehicle and piezoelectric device on the road. To illustrate the idea, the authors considered a fast vehicle moving on an empty road. Whenever a vehicle passes above the piezoelectric model, there are two forces activated at different times. The first activated force occurs when the front tires hit the piezoelectric device while the second activated force occurs when rear tires hit the piezoelectric device. Figure 10 illustrate when each force activated.

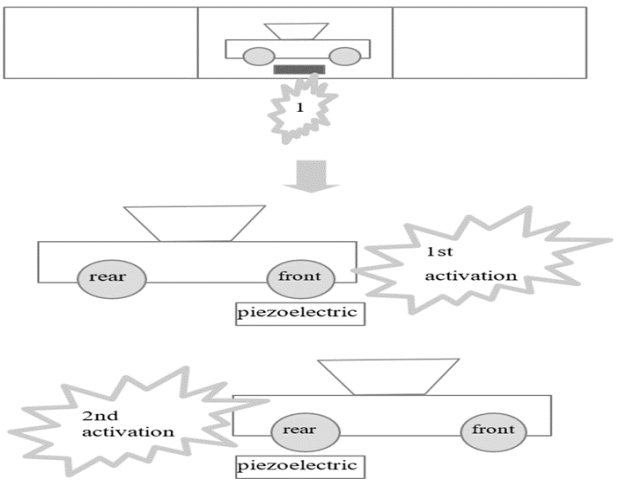

Fig 10. When activated forces occurs

2.5. Integration of Vehicle Dynamic Model , Traffic Model and Piezoelectric Model

The proposed compression based piezoelectric traffic model (CPTM) is based on an integration of three models namely; traffic model, vehicle dynamics model and piezoelectric model. As shown in Fig 11. Firstly, the traffic model receives the arrival rate that defines the traffic flow. After that, the velocity (v) of each vehicle that activates the piezoelectric device is computed. Then the vehicle dynamics model takes the velocity (v) of a vehicle and calculates the vertical force (F) and frequency (f). Finally, the piezoelectric model utilizing the derived the voltage (V) and power (W).

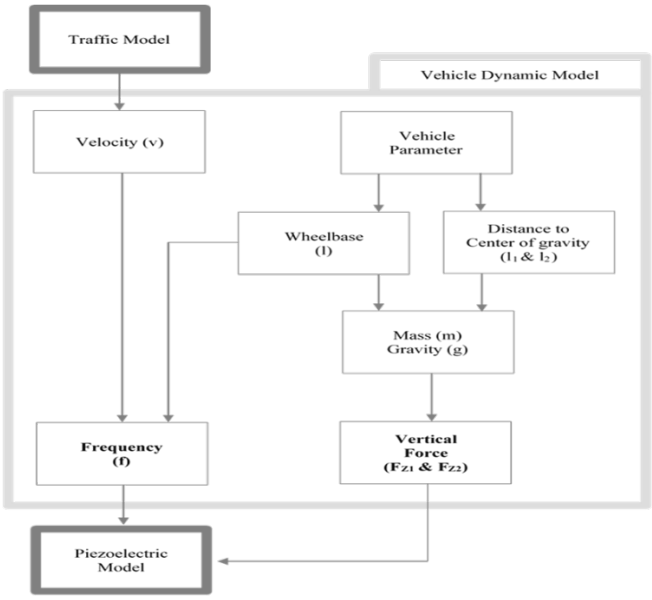

Fig 11. Integration between Vehicle Dynamic Model with Traffic Model and Piezoelectric Model

3. Result and Discussion

In this section, the results are presented and discussed in term of the traffic flow for three different mean arrival rates of λ = 1.0, 0.5 and 0.1. Table 6 illustrates the total number of vehicles and the mean arrival rate. The results show the average number of vehicles for the mean arrival rate (λ) of 1.0 was 7809 over a duration of 180 minutes. By translating this into the traffic flow, it implied that an average of 2603 vehicles/hour or 43.38 vehicles/minute passed through the piezoelectric device. Noticeably, when the mean arrival rate (λ) decreased into 0.5, the average of 5044.25 vehicles activated the piezoelectric for 3 hours whereby the traffic flow is 1681.42 vehicles/hour or 28.02 vehicles/minute. The traffic flow for the mean arrival rate (λ) of 0.1 is 358.75 vehicles/hour or 5.98 vehicles/minute.

Table 6. Total vehicles for the mean arrival rate

Data Set	*Total Vehicle*		
	λ = 1.0	***λ = 0.5***	***λ = 0.1***
1	*7762.0*	*5064*	*1076*
2	*7846.0*	*5009*	*1065*
3	*7771.0*	*5018*	*1060*
4	*7853.0*	*5074*	*1077*
5	*7839.0*	*4993*	*1080*
6	*7777.0*	*5083*	*1089*
7	*7850.0*	*5111*	*1073*
8	*7774.0*	*5002*	*1090*
Average	*7809.00*	*5044.25*	*1076.25*
vehicle / hour	*2603.00*	*1681.42*	*358.75*
vehicle/minute	*43.38*	*28.02*	*5.98*

3.1. Results when Mean Arrival Rate (λ) = 1

The first examination was carried when mean arrival rate (λ) is 1. The obtained result is presented in Fig 12 and Fig 13. The X-axis represents the time in minutes whereas the Y-axis represents the Voltage (V) and the power (W) respectively. It

is clearly shown that the average voltage often fluctuated between 20 V to 50 V. Meanwhile, the total average power ranged between 0.5 mW and 4 mW for almost all tested resistances. In addition, the highest power obtained after 80 minutes. The generated power reached the highest peak of about 4.5 mW, and then immediately fell to the lowest value of approximately 0.5 mW. This is due to the movement of vehicles on a clear road being abruptly greeted by congestion without warning.

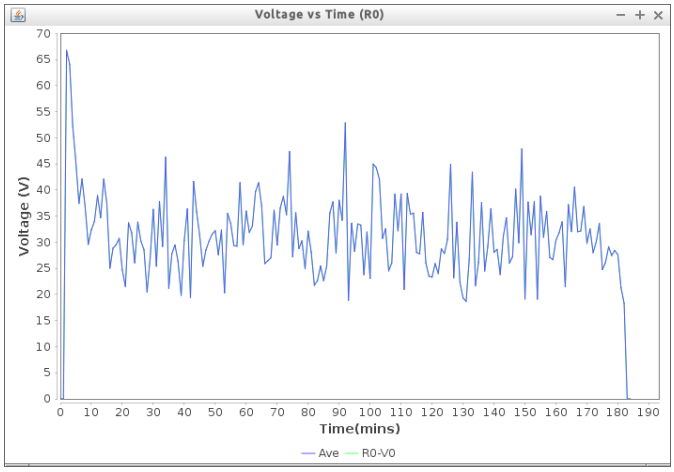

Fig 12. Average Voltage when (λ) = 1 and Resistance (kΩ) = 200

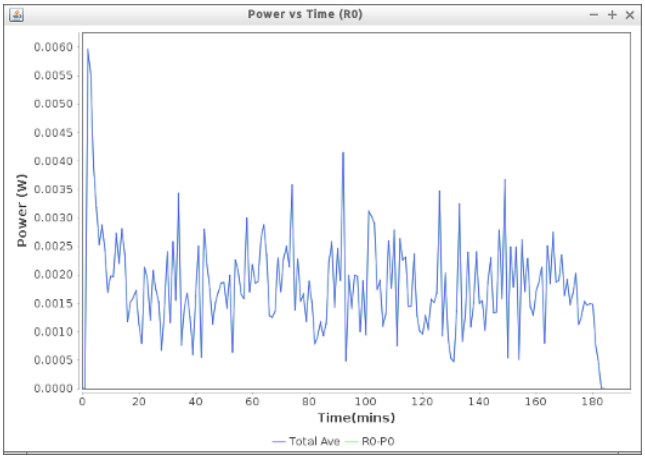

Fig 13. Total Average Power for (λ) = 1 and Resistance = 200 kΩ

3.2. Results when Mean Arrival Rate (λ) = 0.5

The second examination was carried when mean arrival rate (λ) is 0.5. Compared to the previous case, the degree of fluctuation was considerably less than previous one. The range of the average voltage was only 5 V, oscillating mildly between 60 V to 65 V. Therefore, the total average power also fluctuated within a more conservative range of between 4.5 mW and 6 mW. Comparatively, it should also be pointed out that the range of voltage and power for this rate were significantly higher than before. Based on this result, it is noted that the range of the average voltage and total average power for the preceding case were 20 V to 50 V and 0.5 mW to 4 mW, respectively. In effect, the average voltage of Mean arrival rate (λ) = 0.5 was three times higher. The lowest generated power for this rate was 4.5 mW, which is practically higher than the maximum value for the previous case when λ = 1. Figure 14 shows the average power for resistance 200 kΩ.

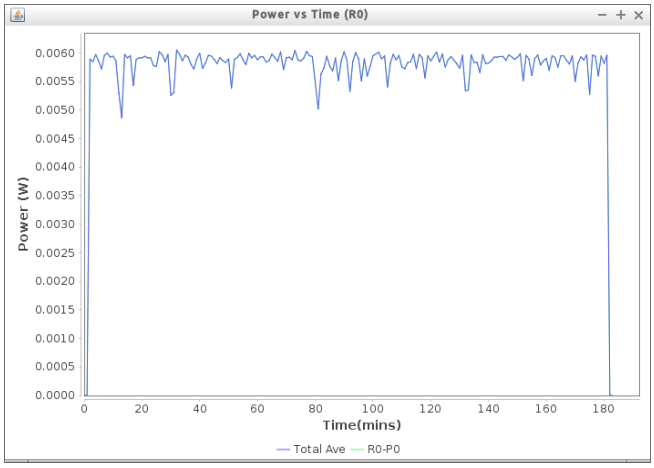

Fig 14. Total Average Power for (λ) = 1 and Resistance = 200 kΩ

3.3. Results when Mean Arrival Rate (λ) = 0.1

The range of the average voltage and total average power fluctuated the least for the mean arrival rate of 0.1. It was noticed from the simulation that the average voltage only vibrated around 60 V most of the time, without any significant bursts or plunges. The same could be said of the total average power. Figure 15 shows the average power for (λ) = 0.1 and resistance = 200 kΩ. Thus, we could claim that around 5.5 mW and 6 mW throughout the duration for all the different variations of resistances. In comparison to the previous means arrival rates, its average voltage and total average power were only slightly lower than the rate of λ = 0.5 but significantly more than λ = 1.0. Therefore, we could expected that the average voltage and power performance lay in between the two. However, the total average power that was exhibited through the collection of figures here did not constitute the total power, but was conclusive as to whether the average performance of power generated would translate into the total performance and vice-versa.

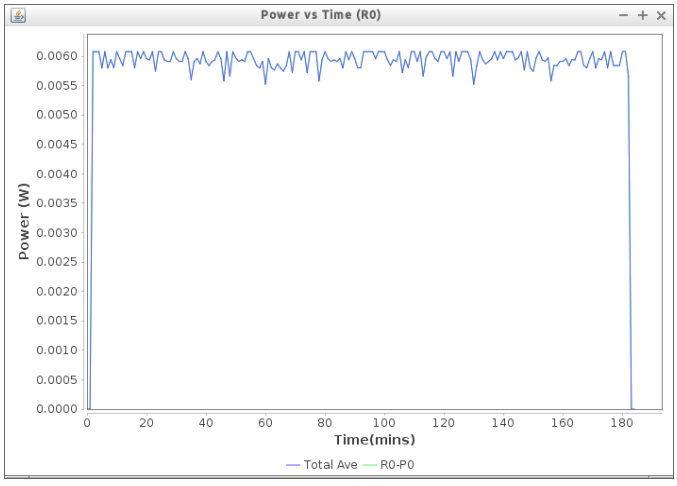

Fig 15. Total Average Power for (λ) = 0.1 and Resistance = 200 kΩ

3.4. Mean Arrival Rate Comparison

In this section, a comparison between the total power generated for the different mean arrival rates (λ) of 1, 0.5, and 0.1, and resistances ranged from 200 (kΩ) to 1600 (kΩ) is performed and presented in Table 7 and Fig 14. On average, the λ value of 0.5 gave the highest power at 29.3961 W, while the λ value of 0.1 generated the lowest power at 6.3915 W. The mean arrival rate (λ) of 1 gave a total power output that was between the highest and lowest power at 13.1790 W. In addition, the total power fluctuated the most and was mostly distinctive when the rate was set at 1.0. This could be observed from the range of the total power between 12.5391 W to 14.1258 W that constituted a difference of 1.5867 W, as opposed to the discrepancy exhibited when the rates were 0.5 and 0.1. The maximum total power differed from one rate to another. For instance, when the mean arrival rate (λ) is 1.0, the maximum total power occurred at 600 kΩ. However, it occurred at 1400 kΩ and 1600 kΩ for the rates of 0.5 and 0.1, respectively. This implied that the resistance could have played a role at mediating the total power for a certain rate.

Table 7. The measurements of the total power for three Mean Arrival Rates at different resistances.

Resistance (kΩ)	Total Power (W)		
	λ =1	λ =0.5	λ =0.1
200	13.7778	29.4968	6.3947
400	12.8926	29.2708	6.3220
600	**14.1258**	29.2634	6.2966
800	12.5391	29.5514	6.3859
1000	12.3109	29.2273	6.4289
1200	13.9838	29.5143	6.4652
1400	12.8668	**29.7460**	6.3698
1600	12.9348	29.0986	**6.4690**
Average	13.1790	29.3961	6.3915

From the Fig 16, it was quite apparent that the generation of total power was optimal when the mean arrival rate was moderate at a value of λ = 0.5. At this rate, the total power generated was quite consistent for numerous resistance values. In fact, the highest total power of 29.7460 W and the lowest one of 29.0986 W only differed by the marginal value of 0.6474 W.

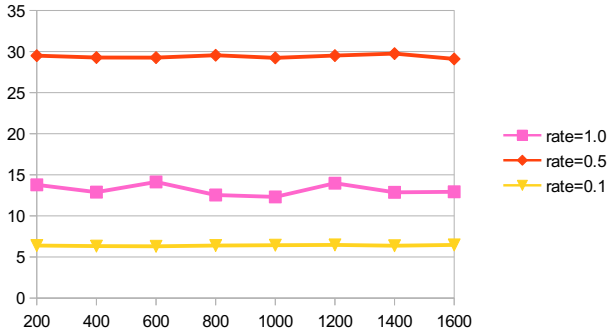

Fig 16. Measurements of the total power for three Mean Arrival Rates at different resistances

4. Discussion

The power generated by a piezoelectric model is significantly affected by the mass and velocity of the vehicle. The velocity of the vehicle is determined by the traffic flow from the traffic model. The relationship can be quite intriguing. High traffic flow usually implies a high movement of vehicles within a specific duration. This, however, does not necessarily imply a high velocity of piezoelectric activation.

For example, when the mean arrival rate is 1 the traffic flow is 43.38 vehicles/minute. And when the number of vehicles is high, the possibility of congestion is high as well. This may force the vehicles to lower their velocity to move in unison. In contrast, when the arrival rate (λ) is 0.1, which was the lowest value in the study, the traffic flow is considerably low at only 5.98 vehicles/minute. However, fewer vehicles imply a lower possibility of congestion. Hence, the vehicles can move freely and activate the piezoelectric device at probably the maximum velocity. The main concerns of constructing a piezoelectric device on the road is finding out the total power generated within a certain period. As such, the key here is to figure out the optimal traffic flow that offers the highest generation of total power. Once the optimal traffic flow is identified, other factors, such as optimal resistance or optimal force, can be easy obtained. At first glance, the graph for the voltage and power generation of the low mean arrival rate seems more promising than that of the higher mean arrival rate. Although the generation of total power varies between one resistance level to another, their differences are rather minute. This is caused by the vacillating frequency of the vehicle that activates the piezoelectric device. Unlike the lab setting, where a constant excitation at the same frequency is ensured, the real-life setting involves an ongoing fluctuation of activation frequencies. The recurring fluctuation of frequencies enforced by passing vehicles in traffic is collectively dilute the role of the resistance in the piezoelectric model with respect to the optimization of the generation of voltage, and consequently, the total power. However, in cases where the traffic flow is high, as exhibited by the mean arrival rate of 1.0, the mediation of resistance is still significant. Therefore, the impact of resistance in terms of traffic flow can be beneficial to the optimization of the piezoelectric device. When the traffic flow is high, the resistance should be adjusted to 600 kΩ or 1200 kΩ to enable the highest generation of total power for the piezoelectric entity. On the other hand, when the traffic flow is moderate or low, the resistance can be left unchanged. Rationally, the total power depends on two factors. First, the velocity at which most vehicles pass through the piezoelectric device, and second, the total number of vehicles that activate the piezoelectric device within a duration. In combination, the interplay of these two factors determines the generation of total power at the piezoelectric entity. At the highest mean arrival rate (λ) of 1.0, the traffic density was very high, and congestion happened quite frequently. As such, the velocity of the vehicles was mostly low when they passed the piezoelectric device. This was detrimental to the first factor. Despite the high number of total vehicles that occupied the road, the boost from this second factor did not maximize the generation of total power. And when the mean arrival rate (λ) was lowest at 0.1, the traffic flow was very low as well. Given that not many vehicles were

occupying the road, nearly all the vehicles were able to move at a maximum velocity. This ensured the maximization of the first factor. However, at this rate, the total number of vehicles suffered, plunging the second factor into a nadir. In effect, the total power generated was the lowest. The total power generated was optimal when the mean arrival rate (λ) was 0.5. This could be attributed to the right balance between the traffic flow and the total number of vehicles. When the traffic flow was moderate, the velocity of each vehicle that passed the piezoelectric device was consistently high. In addition, the total number of vehicles was also maintained at a high level. Thus, the total power was maximized.

5. Conclusion

This research has been conducted to examine the probability of harvesting the power from traffic road applications. The study proposed using piezoelectric device which used to generate electric energy form traffic roads. The experiments were conducted at three different average arrival rates as λ equals to .01, 0.5, and 1.0. The proposed piezoelectric harvester's electrical power scavenging capacity not only depends on the harvester but also on the external electrical load as well. For a given exciting vibration, there is an optimal electrical load, with the maximum value, in terms of harvesting, can be achieved by electrical power harvester. The obtained results show that, a maximum total power of 29.746 Watts was harvested at λ=0.5. The results also revealed that when the resistance was set as 600 kΩ or 1,200 kΩ, harvesting of the optimum total power could be achieved. The harvested power and voltage could be sufficient for the use of common appliances such as lighting, communication equipment and roadside billboards , if multiple arrays of PCT planted along the roads.

6. Acknowledgement

The authors gratefully acknowledged the financial support by the Ministry of Higher Education Malaysia under ERGS research grant with the vote number of E035 for this research works. The authors wish to express their heartfelt appreciativeness to Office for Research, Innovation, Commercialization and Consultancy Management (ORICC), UTHM for their continuous support and assistance in managing the research grant.

References

[1] Vatansever, D., E. Siores, R.L. Hadimani, and T. Shah, Smart woven fabrics in renewable energy generation. 2011: INTECH Open Access Publisher.

[2] Vatansever, D., E. Siores, and T. Shah, Alternative Resources for Renewable Energy: Piezoelectric and Photovoltaic Smart Structures. Global Warming - Impacts and Future Perspective 2012: p. 263.

[3] Oy, S.A. and A.E. Özdemir. Usage of piezoelectric material and generating electricity. in Renewable Energy Research and Applications (ICRERA), 2016 IEEE International Conference on. 2016. IEEE.

[4] Mitcheson, P.D., E.M. Yeatman, G.K. Rao, A.S. Holmes, and T.C. Green, Energy harvesting from human and machine motion for wireless electronic devices. Proceedings of the IEEE, 2008. 96(9): p. 1457-1486.

[5] Beeby, S.P., M.J. Tudor, and N. White, Energy harvesting vibration sources for microsystems applications. Measurement science and technology, 2006. 17(12): p. R175.

[6] Starner, T., Human-powered wearable computing. IBM systems Journal, 1996. 35(3.4): p. 618-629.

[7] Roundy, S., P.K. Wright, and J. Rabaey, A study of low level vibrations as a power source for wireless sensor nodes. Computer communications, 2003. 26(11): p. 1131-1144.

[8] Dayou, J. and M.S. Chow, Performance study of piezoelectric energy harvesting to flash a LED. International Journal of Renewable Energy Research (IJRER), 2012. 1(4): p. 323-332.

[9] Özdemır, A.E. and S.A. Oy. Alternative renewable energy producing systems by utilizing piezoelectric transducers. in Renewable Energy Research and Applications (ICRERA), 2016 IEEE International Conference on. 2016. IEEE.

[10] Viola, F., P. Romano, R. Miceli, and G. Acciari. On the harvest of rainfall energy by means of piezoelectric transducer. in 2013 International Conference on Renewable Energy Research and Applications (ICRERA). 2013. IEEE.

[11] Williams, C. and R.B. Yates, Analysis of a micro-electric generator for microsystems. Sensors and Actuators A: Physical, 1996. 52(1-3): p. 8-11.

[12] Tichý, J., J.r. Erhart, E. Kittinger, and J. Prívratská, Fundamentals of piezoelectric sensorics: mechanical, dielectric, and thermodynamical properties of piezoelectric materials. 2010: Springer Science & Business Media.

[13] Kompis, C. and S. Aliwell, Energy harvesting technologies to enable remote and wireless sensing. Sensors and Instrumentation-Knowledge Transfer Network, 2008.

[14] Ali, S.F., M. Friswell, and S. Adhikari, Analysis of energy harvesters for highway bridges. Journal of Intelligent Material Systems and Structures, 2011: p. 1929.

[15] Gusarov, B., E. Gusarova, B. Viala, L. Gimeno, S. Boisseau, O. Cugat, E. Vandelle, and B. Louison, Thermal energy harvesting by piezoelectric PVDF polymer coupled with shape memory alloy. Sensors and Actuators A: Physical, 2016. 243: p. 175-181.

[16] Botteron, C., D. Briand, B. Mishra, G. Tasselli, P. Janphuang, F.-J. Haug, A. Skrivervik, R. Lockhart, C. Robert, and N.F. de Rooij, A low-cost UWB sensor node powered by a piezoelectric harvester or solar

cells. Sensors and Actuators A: Physical, 2016. 239: p. 127-136.

[17] Zhao, J., J. Yang, Z. Lin, N. Zhao, J. Liu, Y. Wen, and P. Li, An arc-shaped piezoelectric generator for multi-directional wind energy harvesting. Sensors and Actuators A: Physical, 2015. 236: p. 173-179.

[18] Taghadosi, M., L. Albasha, N. Qaddoumi, and M. Ali, Miniaturised printed elliptical nested fractal multiband antenna for energy harvesting applications. IET Microwaves, Antennas & Propagation, 2015. 9(10): p. 1045-1053.

[19] Camarda, A., A. Romani, E. Macrelli, and M. Tartagni, A 32 mV/69 mV input voltage booster based on a piezoelectric transformer for energy harvesting applications. Sensors and Actuators A: Physical, 2015. 232: p. 341-352.

[20] Cheng, T.H., K.B. Ching, C. Uttraphan, and Y.M. Heong, A Review on Energy Harvesting Potential from Living Plants: Future Energy Resource. International Journal of Renewable Energy Research (IJRER), 2018. 8(4): p. 2398-2414.

[21] Colak, I. and E. Kabalci, Implementation of energy-efficient inverter for renewable energy sources. Electric Power Components and Systems, 2013. 41(1): p. 31-46.

[22] Sakagami, T., Y. Shimizu, and H. Kitano. Exchangeable batteries for micro EVs and renewable energy. in Renewable Energy Research and Applications (ICRERA), 2017 IEEE 6th International Conference on. 2017. IEEE.

[23] Lawan, M., J. Raharijaona, M. Camara, and B. Dakyo. Power control for decentralized energy production system based on the renewable energies—using battery to compensate the wind/load/PV power fluctuations. in Renewable Energy Research and Applications (ICRERA), 2017 IEEE 6th International Conference on. 2017. IEEE.

[24] Chalasani, S. and J.M. Conrad. A survey of energy harvesting sources for embedded systems. in Southeastcon, 2008. IEEE. 2008. IEEE.

[25] Jiang, X., Y. Li, J. Wang, and J. Li, Electromechanical modeling and experimental analysis of a compression-based piezoelectric vibration energy harvester. International Journal of Smart and Nano Materials, 2014. 5(3): p. 152-168.

[26] Vassiliadis, S., Advances in Modern Woven Fabrics Technology. 2011, [Place of publication not identified]: INTECH.

[27] Aldraihem, O. and A. Baz, Energy harvester with a dynamic magnifier. Journal of Intelligent Material Systems and Structures, 2011. 22(6): p. 521-530.

[28] Tang, L. and Y. Yang, A multiple-degree-of-freedom piezoelectric energy harvesting model. Journal of Intelligent Material Systems and Structures, 2012. 23(14): p. 1631-1647.

[29] Wu, H., L. Tang, P.V. Avvari, Y. Yang, and C.K. Soh. Broadband energy harvesting using nonlinear 2-DOF configuration. in SPIE Smart Structures and Materials+ Nondestructive Evaluation and Health Monitoring. 2013. International Society for Optics and Photonics.

[30] Peigney, M. and D. Siegert, Piezoelectric energy harvesting from traffic-induced bridge vibrations. Smart Materials and Structures, 2013. 22(9): p. 095019.

[31] Jiang, X., Y. Li, J. Li, J. Wang, and J. Yao, Piezoelectric energy harvesting from traffic-induced pavement vibrations. Journal of Renewable and Sustainable Energy, 2014. 6(4): p. 043110.

[32] Zhang, Y., S.C. Cai, and L. Deng, Piezoelectric-based energy harvesting in bridge systems. Journal of Intelligent Material Systems and Structures, 2014. 25(12): p. 1414-1428.

[33] Yang, C.H., M.S. Woo, Y. Song, J.H. Eom, J.H. Kim, G.J. Song, S.K. Hong, T.H. Sung, J.Y. Choi, and S.K. Ryu. Development of impact-based piezoelectric road energy harvester for practical application. in Renewable Energy Research and Applications (ICRERA), 2016 IEEE International Conference on. 2016. IEEE.

[34] Thong, K.T., B. Kok, C. Uttraphan, S. Gareh, and Z.J. Sam. Data acquisition system for Piezoelectric Cymbal Transducer energy harvesting. in 2016 IEEE International Conference on Power and Energy (PECon). 2016. IEEE.

[35] Barsoum, M. and M. Barsoum, Fundamentals of ceramics. 2002: CRC press.

[36] Gareh, S., B. Kok, C. Uttraphan, K. Thong, and A. Borhana. Evaluation of piezoelectric energy harvester outcomes in road traffic applications. in 4th IET Clean Energy and Technology Conference (CEAT 2016). 2016. IET.

[37] Kok, B.C., S. Gareh, H.H. Goh, and C. Uttraphan, Electromechanical-Traffic Model of Compression-Based Piezoelectric Energy Harvesting. MATEC Web Conf., 2016. 70: p. 10007.

[38] Nagel, K. and M. Schreckenberg, A cellular automaton model for freeway traffic. Journal de physique I, 1992. 2(12): p. 2221-2229.

[39] Bain, N., T. Emig, F.-J. Ulm, and M. Schreckenberg, Velocity statistics of the Nagel-Schreckenberg model. Physical Review E, 2016. 93(2): p. 022305.

[40] Guidolin, M., A.S. Chen, B. Ghimire, E.C. Keedwell, S. Djordjević, and D.A. Savić, A weighted cellular automata 2D inundation model for rapid flood analysis. Environmental Modelling & Software, 2016. 84: p. 378-394.

[41] Jazar, R.N., Vehicle dynamics: theory and application. 2013: Springer Science & Business Media.

[42] Abdullah, M., J. Jamil, and M. Salim. Dynamic performances analysis of a real vehicle driving. in IOP Conference Series: Materials Science and Engineering. 2015. IOP Publishing.

[43] Toledo, B., M. Sanjuan, V. Muñoz, J. Rogan, and J. Valdivia, Non-smooth transitions in a simple city traffic model analyzed through supertracks. Communications in Nonlinear Science and Numerical Simulation, 2013. 18(1): p. 81-88.